Neural networks for predicting kerf characteristics of CO_2 laser-machined FFF PLA/WF plates

N. A. Fountas[1] [0000-0001-5859-6503], K. Ninikas[2] [0000-0002-1304-3363], D. Chaidas[2] [0000-0002-5349-9613], J. Kechagias[2] [0000-0002-5768-4285] and N. M. Vaxevanidis[1]* [0000-0002-7641-5267]

[1] Laboratory of Manufacturing Processes and Machine Tools (LMProMaT), Department of Mechanical Engineering Educators, School of Pedagogical and Technological Education (ASPETE), Amarousion, GR 151 22, Greece.
[2] School of Technology, University of Thessaly, Karditsa, GR 43100, Greece

*Corresponding author: vaxev@aspete.gr

Abstract. The current work is a follow-up of previous research published by the authors and investigates the effect of CO_2 laser cutting with variable cutting parameters of thin 3D printed wood flour mixed with poly-lactic-acid (PLA/WF) plates on kerf angle (KA) and mean surface roughness (Ra). The full factorial experiments previously conducted, followed a custom response surface methodology (RSM) to formulate a continuous search domain for statistical analysis. Cutting direction, standoff distance, travel speed and beam power were the independent process parameters with mixed levels, resulting to a set of 24 experiments. The 24 experiments were repeated three times giving a total of 72 experimental tryouts. The results analyzed using analysis of variance (ANOVA) and regression, to study the synergy and effect of the parameters on the responses. Thereby, several neural network topologies were tested to achieve the best results and find a suitable neural network to correlate inputs and outputs, thus; contributing to related academic research and actual industrial applications.

Keywords: CO_2 laser cutting, 3D Printing, PLA wood flour, analysis of variance, neural networks.

1 Introduction.

Laser beam machining (LBM) is a non-traditional process that can achieve high dimensional accuracy, surface quality, and process efficiency [1]. A laser beam can apply cutting, milling, turning, drilling, etching, and welding [2,3]. Laser processing is applied in many materials, i.e., in metals [4], thermo-plastics [5], composites [6], and 3D printed materials [7-10], to name a few. In literature, a continuous-wave, low-power CO_2 laser cutting has been used efficiently on sheet-form thermoplastic materials [11-15]. Driving parameters for the machinability performance of laser cutting process are: (i) the beam parameters including the beam power (BP), the frequency, the TEM mode, and the spot radius; (ii) the focal parameters including the focal distance, the orifice diameter, the stand-off distance, the assist-gas pressure and the spot radius at the upper cut-surface, (iii) the cut material parameters such as surface texture, absorptivity, thickness, thermal and physical properties, and finally, (iv) the machine parameters including

the mechanical elements, the type of assist-gas, the orifice type, the laser travel velocity, etc. [11]. Kerf profile (Kerf), cut average surface roughness (Ra), heat-affected zone (HAZ) and material removal rate (MRR) is considered crucial attributes that are investigated the most [16, 17].

Fused Filament Fabrication (FFF) is a widely-applied 3D printing method for low-cost production of physical final parts and prototypes [18]. Dimensional accuracy and surface quality are the two main concerns of the FFF process that need improvement [19, 20]. This is even more notable by using the low-cost FFF 3D printers where it is complicated to be achieved good shape characteristics such as circle or cuboid edges and small details like pines or pillows [21]. Hybrid methods that combine the 3D printing process shape flexibility and dimensional accuracy of the material removal processes are investigated in literature as an alternative. For this purpose, a laser beam process can be considered a post-processing method for improving the FFF parts quality. Kechagias et al. [9] experimented with the combination of FFF 3D printed plates and laser cutting. They 3D-printed 4mm pure PLA plates and cut them using a continuous-wave CO_2 Laser. It is found that the parallel and vertical cuts had different mean values and spread for both the kerf angle and surface roughness performance characteristics. They used beam power between 82.5 and 97.5 W and laser travel speed between 8 and 18 mm/s. The kerf angles were between 0.884 and 1.612 degrees, and the Ra values were 0.81 to 6.193μm. These values are very close to them, achieved by cutting pure PMMA materials [5] and better than 12.84 - 21.77 μm achieved by the FFF-3D printing process [8-10]. There are many recent works regarding laser cutting of thin thermoplastic materials, but very few concerning 3D printed materials [7-10]. However, the 3D printed thin plates of organic, eco-friendly composite materials combined with laser processing could be an alternative for low-cost tailored products and assemblies [22-24]. Furthermore, the systematic investigation of the influence of the deposition angle during laser cutting of PLA with wood flour filler (PLA/WF) plates is investigated for the first time. Organic materials such as PLA mixed with wood flour (PLA/WF) are available nowadays in various mixtures of WF and PLA [25]. The PLA/WF composite material has an echo-friendly profile and a wooden appearance [26].

The purpose of this research is to further investigate the machinability of the PLA with wood floor printed plates during the laser cutting of a continuous-wave low-power CO_2 laser. The kerf angle (KA, degrees) and mean surface roughness Ra (μm) were measured under a range of different cutting directions and conditions. Three cutting directions (CD: 0^o, 45^o, 90^o), two stand-off distances (SoD: 7 and 8 mm), three beam travel speeds (TS: 8, 13, and 18 mm/s), and four laser beam powers (BP: 82.5, 90, 97.5 and 105 W) were examined. Consequently a total of 72 cuts were performed to achieve all the possible parameter's level combinations according to the full factorial design. Following that, a continuous experimental search domain was formulated using a custom response surface design. The results were statistically analyzed whereas several neural network topologies were tested to end up with the best predictive network for practical applications.

2 Experimental results.

Three thin plates (X, Y, Z: 100 X 20 X 4 mm) were manufactured using an FFF 3DP process. The FFF 3D printer was *Craftbot® Plus*. The PLA/WF material used for this experiment was the *NEEMA3D™ WOODPLUS* (30% WF; 70% PLA; 1.1-1.2 g/cm^3; 140-150^{o}C melting range; 1.75 mm filament). The printing head nozzle diameter was 0.4 mm, while the printing temperature was set at 200^{o}C—the bed temperature was set at 60^{o}C. The three 4 mm plates were printed

with 100% infill density (one top layer, one bottom layer, one shell, 0.3 mm layer thickness, 13 layers in total, 40mm/s printing speed, 9.51 gr weight). Finally, the three different raster deposition angles (0°, 45°, and 90°) were measured from the X-axis (100mm in length). A continuous-wave CO_2 laser *BCL 1325B* with a 10.6 μm wavelength and 2mm tip diameter was used. *RDWorks® v. 8.0* software environment is used for the laser-cut design. The parameters' values are concluded after an extensive literature survey, preliminary experimental work, and previous publications [5, 9]. Two levels of stand-off distance (SoD: 7 and 8 mm), three levels of travel speed (TS: 8, 13, and 18 mm/s), and four levels of beam power (BP: 82.5, 90, 97.5, and 105 W) are finally selected. In this experimental space and for the specific material cutting, the airflow pressure kept constant at 1 bar. The manufacturer's focal length is fixed at 46 mm. The laser beam focal spot is about 0.4 mm when the SoD is 8 mm from the upper surface. Changing the SoD, the spot diameter and the airflow distribution at the upper surface also change. All three plates before cutting had the same orientation in the laser bed.

Full factorial experimental design methodology is selected. All twenty-four experiments were repeated three times for the three PLA/WF plates (DA: 0°, 45°, and 90° from the X-axis, respectively) resulting to a total of 72 results. Fig.1a shows the laser-cut procedure on the three PLA/WF plates with the total of 72 cuts (Fig.1b). The laser is adjusted to perform all cuts in Y-axis; when DA (deposition angle) is 90° while laser CD (cutting direction) is zero, therefore parallel with the filament.

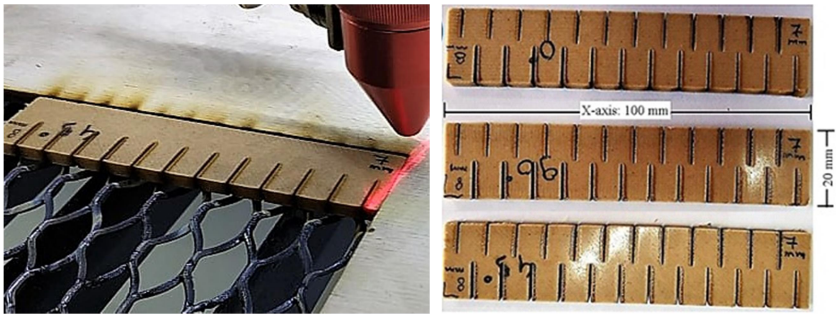

Fig. 1. Experimental work: (a) Cutting procedure, and (b) Seventy-two cuts.

Table 1 presents the cutting parameters and their levels.

Table 1. Parameters and levels based on the full factorial design of experiments.

Full factorial design of experiments						
Parameter	Symbol	Level				
		1	2	3	4	Unit
Stand-off Distance	SoD	7	8	-	-	mm
Travel Speed	TS	8	13	18	-	mm/sec
Beam Power	BP	82.5	90.0	97.5	105	W
Cutting Direction	CD	0	45	90	-	(deg.)

Measurements for upper and down kerf widths (W_u, W_d) were taken using a digital microscope (*Cooling Tech®*, Fig.2a). Thereby, kerf angle *KA* was calculated using Eq.1.

$$KA = \tan^{-1}\left(\frac{W_u - W_d}{2 \times d}\right) \quad (1)$$

where, *d* is the thickness for the plates; 4mm.

Surface roughness *Ra* was measured with the *Surftest® SJ-210* profilometer (Fig.2b). To measure Ra, each plate was separated into twenty-four smaller items (Fig.2c).

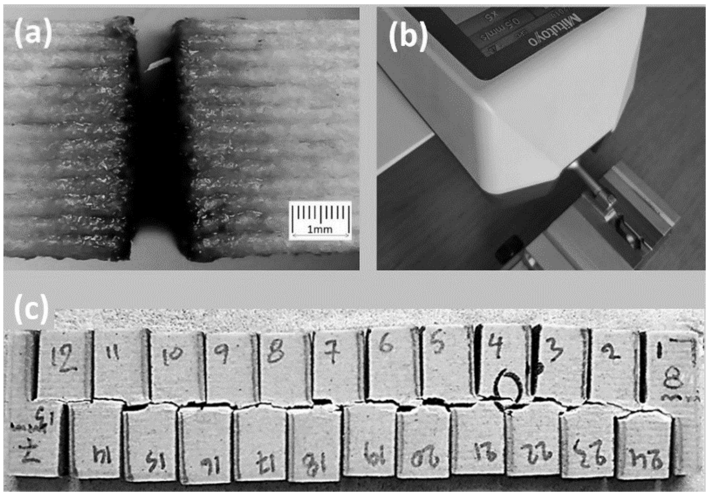

Fig. 2. Measurements: (a) kerf geometry, (b) roughness measurements and (c) smaller pieces for the Ra measurements.

Table 2 tabulates the experimental results for *KA* and *Ra* objectives along with corresponding readings of upper width (W_u, mm) and down width (W_d, mm) for the cuts performed on the three plates.

Table 2. Experimental results.

	Input parameters			Output parameters					
				0 deg		45 deg		90 deg	
No	SoD (mm)	TS (mm/s)	LP (W)	KA (deg)	Ra (μm)	KA (deg)	Ra (μm)	KA (deg)	Ra (μm)
1	7	8	82.5	0.136	17.392	0.351	18.8	-0.186	15.104
2	7	8	90	-1.454	23.12	-1.668	22.064	-1.318	20.032
3	7	8	97.5	-1.611	21.296	-2.226	21.136	-1.783	20.368
4	7	8	105	-0.695	21.136	-0.695	20.496	-0.902	15.68
5	7	13	82.5	-0.616	28.08	-0.695	29.77	-0.974	26.78
6	7	13	90	0.623	24.986	-0.759	28.028	-0.143	22.724
7	7	13	97.5	-0.623	30.55	-0.695	26.234	0.695	22.23
8	7	13	105	-0.165	29.874	-0.888	30.524	-1.174	24.492
9	7	18	82.5	0.623	31.788	0.63	29.016	0.279	23.796
10	7	18	90	0.788	31.248	0.279	30.06	0.695	23.796
11	7	18	97.5	0.695	33.516	0.423	29.412	0.208	25.524
12	7	18	105	1.06	29.088	0.895	28.332	0.831	23.76
13	8	8	82.5	-0.136	22.672	-0.136	19.568	-0.107	22.96
14	8	8	90	-0.838	23.92	-0.666	23.504	-0.193	23.408
15	8	8	97.5	-0.279	23.92	-0.945	23.872	-0.709	24.496
16	8	8	105	0.093	22.256	-0.559	23.296	-0.007	22.672
17	8	13	82.5	0.623	30.55	0.208	31.538	0.809	33.722
18	8	13	90	1.01	29.562	0.143	29.796	0.831	31.304
19	8	13	97.5	0.594	28.938	0.072	31.564	0.444	30.368

20	8	13	105	0.279	26.338	0.072	28.028	0.351	30.55
21	8	18	82.5	1.468	30.996	1.733	33.264	1.182	36.036
22	8	18	90	1.117	29.304	1.246	29.376	0.917	34.632
23	8	18	97.5	0.637	27.54	1.318	28.368	0.824	32.796
24	8	18	105	0.881	30.276	1.01	29.196	0.63	31.104

3 Statistical analysis.

To enable a suitable experimental region with continuous independent parameters for response prediction, the initial full factorial design was turned to a customized response surface design with the same number of experiments and standard parameters. Thereby, the results referring to *KA* and *Ra* were statistically examined through Analysis of Variance (ANOVA), to study the significance of independent parameters. Contour plots (Fig.3) were created to interpret the effects between two pairs of parameters, thus; allowing for more accurate and rigorous representation [27]. Pairs of independent parameters were decided based on their effect hierarchy, i.e.; for kerf angle KA, TS and SoD are the most influential ones, followed by CD and BP. Similarly for Ra, CD and TS are the most influential ones, followed by SoD and BP.

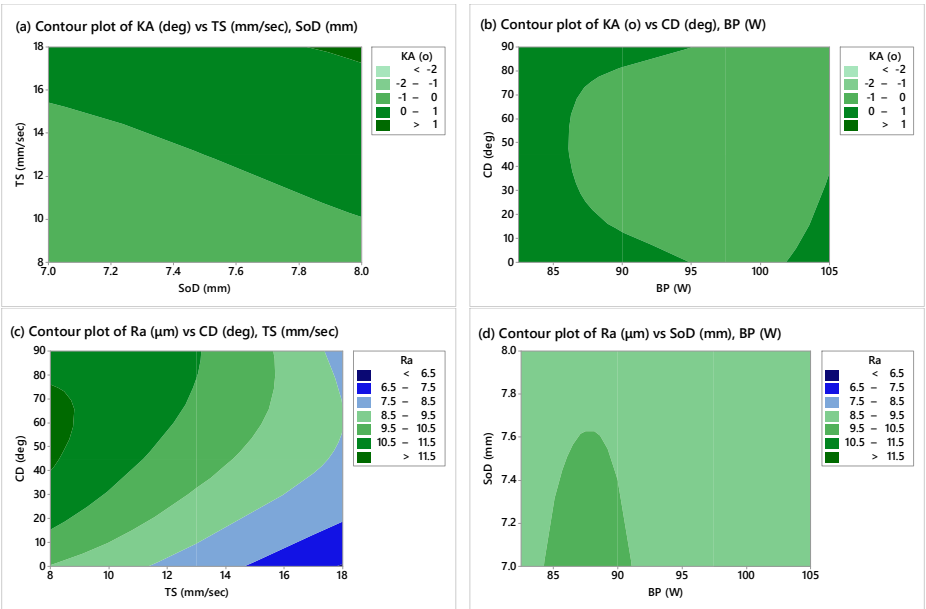

Fig. 3. Contour plots for examining the effect of CO_2 laser cutting parameters to: (a) Kerf angle KA, vs TS, SoD; (b) KA vs CD, BP; (c) Ra vs CD, TS; (d) Ra vs SoD, BP.

Fig.3a depicts the contour plot for kerf angle KA variation in terms of the two most influential parameters; TS and SoD. Since kerf angle should be minimized, it can be observed that an advantageous region for parameter settings is the pale-green contour area in the plot. This region suggests that KA may be maintained close to zero for the entire range of SoD settings, provided that TS is between 8-15.5 mm/s. By examining Fig.3b, it is observed that KA is main-

tained to low values when BP is adjusted to a value range between 86-105W. However CD should be adjusted to moderate levels, i.e., 30-70deg. By examining Fig.3c where Ra variation in terms of CD and TS is illustrated, it is shown that Ra is dramatically minimized when setting high travel speed values (14.5-18 mm/s) under low cutting direction degrees (0-15deg). Fig.3d shows that Ra can be maintained at low levels by setting any value for SoD. However a small region for BP between 85-90W should be avoided since this range of setting may increase roughness if SoD is to be set between 7-7.6mm.

4 Neural network prediction.

A number of different Artificial neural network (ANN) architectures (feed-forward, back propagation) were tested for predicting the responses of kerf angle *KA* and surface roughness *Ra*. In the analysis, the four independent variables cutting direction CD, stand-off distance SoD, travel speed TS and beam power BP were considered as the input variables for the ANN. Each of these parameters has been characterized by one neuron, thus, the input layer in the ANN structure had four neurons. The database has been built considering the series of CO_2 laser cutting experiments at the limit ranges of each independent variable. Experimental results for kerf angle and surface roughness were used to train the ANN to investigate the input–output correlations. The database was then divided into two categories, namely the training category which has been exclusively used to adjust the network weights and the test category, which corresponds to the set that validates the results of the training protocol [28, 29]. Neural network training involved updating the weights of the connections in such a manner that the error between the network's outputs and the actual output is minimized. To determine the number of neurons in the single hidden layer selected, different network structures with varying number of neurons in the hidden layer were tested [30, 31]. After training, the topology 4-12-2 was finally selected as the optimum (Fig.4)

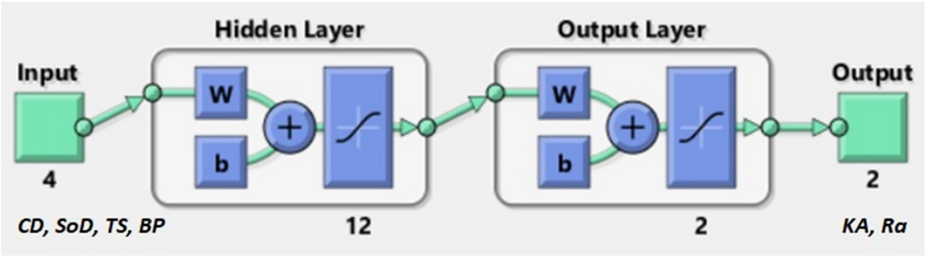

Fig. 4. ANN architecture with four inputs, one hidden layer (12 neurons) and two outputs.

The activation level of neurons was determined by tan–sigmoid transfer function except for output layer neurons for which linear output transfer function was used so that output is not limited to small values. The ANN was simulated in *MATLAB® 2014b*. In order to evaluate the competence of this trained network, the training data set was presented to the trained network. Mean squared error (MSE) in ANNs is the average squared difference between network output values and target values [32]. For the network implemented in the study, best validation performance was equal to 0.25907 at epoch 5 (Fig. 5). Fig. 6 shows the regression analysis results between the network response and the corresponding targets. High correlation coefficient (R-value) between predicted results (outputs) and targets validated the performance of the ANN implemented. Regression values measure the correlation between output values and targets. The

results acquired for this study shown a good correlation among output values and targets during training (R=0.995), validation (R=0.993), and testing (R=0.993). Based on these outputs it is proven that the trained ANN is accurate for modeling the non-linearity presented in the experimental domain for laser cutting, at least when it comes to FFF PLA/WF material.

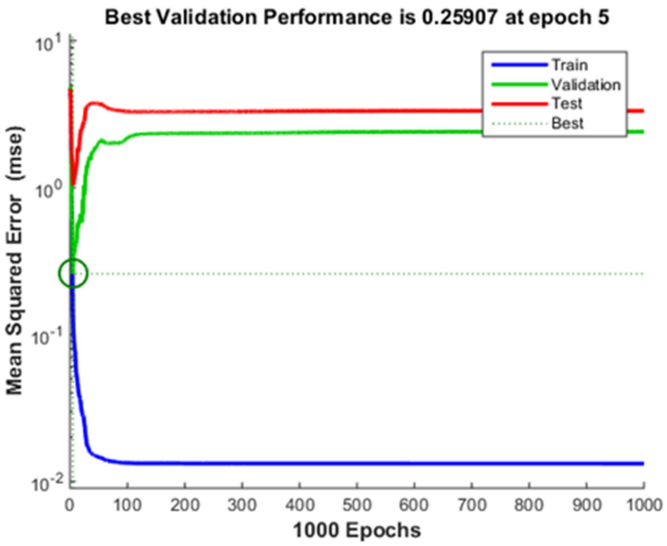

Fig. 5. Best validation performance for the ANN implemented.

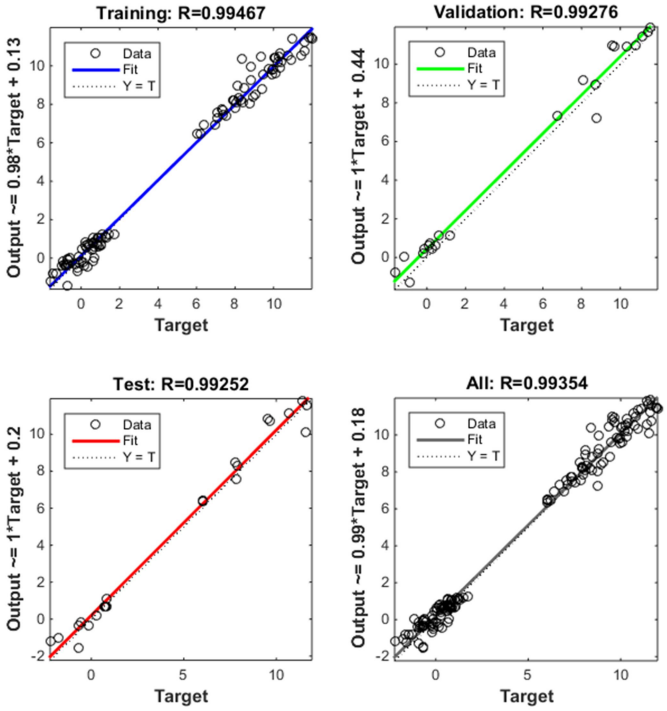

Fig. 6. Regression plots for ANN performance verification.

5 Conclusions.

This work examined the effect of four essential parameters, namely cutting direction, standoff distance, travel speed and beam power on the responses, of kerf angle and surface roughness when it comes to CO_2 laser cutting of 3D-printed PLA with wood flour plates with 4 mm thickness. Laser cutting experiments have been established following the full factorial multi-level design concept resulting to 24 experiments per cutting direction. This led to a total of 72 series of experiments that statistically examined after creating a custom response surface design. To investigate non-linearity and parameter effects on the two responses, statistical analysis involved contour plots. Finally the responses were modelled using a back-propagation neural network after testing several architectures with altered topologies in the hidden layer. It was shown that the final ANN architecture adopted, can accurately predict experimental results for laser cutting the PLA with wood flour material, in terms of kerf angle and surface roughness. As a future work authors plan to implement different evolutionary algorithms and optimize the CO_2 laser cutting of PLA/WF material by formulating a multi-objective optimization problem and having either the ANN, or robust full quadratic regression models under the role of objective functions. Moreover, other 3D-printing filament materials of great importance to industrial applications are to be experimentally investigated for characterizing the process and optimizing its control parameters.

Acknowledgments

The authors acknowledge the financial support for the dissemination of this work provided by the Special Account for Research of ASPETE (ELKE) through the funding program "*Strengthening ASPETE's research*".

References

1. Yilbas BS. Study of Parameters for CO2 Laser Cutting Process. Materials and Manufacturing Processes. 1998;13:517–536.
2. Chryssolouris G. Laser machining: theory and practice. Springer Science & Business Media. Springer Science & Business Media; 2013.
3. Sudha C, Parameswaran P, Krishnan R, et al. Effect of Laser Shock Processing on the Microstructure of 304(L) Austenitic Stainless Steel. Materials and Manufacturing Processes. 2010;25:956–964.
4. Rajamani D, Siva Kumar M, Balasubramanian E, Tamilarasan A (2021) Nd: YAG laser cutting of Hastelloy C276: ANFIS modeling and optimization through WOA. Materials and Manufacturing Processes 36:1746–1760. https://doi.org/10.1080/10426914.2021.1942910
5. Kechagias, J.D., Ninikas, K., Stavropoulos, P. et al. A Generalised Approach on Kerf Geometry Prediction during CO2 Laser cut of PMMA Thin Plates using Neural Networks. Lasers Manuf. Mater. Process. 8, 372–393 (2021). https://doi.org/10.1007/s40516-021-00152-4
6. Hu J, Zhu D. Experimental study on the picosecond pulsed laser cutting of carbon fiber-reinforced plastics. Journal of Reinforced Plastics and Composites. 2018;37:993–1003.
7. Moradi M, Karami Moghadam M, Shamsborhan M, et al. Post-Processing of FDM 3D-Printed Polylactic Acid Parts by Laser Beam Cutting. Polymers. 2020;12.
8. Kechagias JD, Ninikas K, Petousis M, et al. An investigation of surface quality characteristics of 3D printed PLA plates cut by CO2 laser using experimental design. Mater Manuf Process. 2021;36:1544–1553.
9. Kechagias JD, Ninikas K, Petousis M, et al. Laser cutting of 3D printed acrylonitrile butadiene styrene plates for dimensional and surface roughness optimization. The International Journal of Advanced Manufacturing Technology. 2021;
10. Kechagias JD, Fountas NA, Ninikas K, et al. Surface characteristics investigation of 3D-printed PET-G plates during CO2 laser cutting. Mater Manuf Process. 2021;1–11.
11. Yue TM, Lau WS. Pulsed Nd:YAG Laser Cutting of Al/Li/SiC Metal Matrix Composites. Materials and Manufacturing Processes. 1996;11:17–29.
12. Atanasov PA, Baeva MG. CW CO 2 laser cutting of plastics. XI International Symposium on Gas Flow and Chemical Lasers and High-Power Laser Conference. 1997.
13. Zhou BH, Mahdavian SM. Experimental and theoretical analyses of cutting nonmetallic materials by low power CO2-laser. Journal of Materials Processing Technology. 2004;146:188–192.
14. Madić M, Petrović G, Petković D, et al (2022) Application of a Robust Decision-Making Rule for Comprehensive Assessment of Laser Cutting Conditions and Performance. Machines 10:153. https://doi.org/10.3390/machines10020153
15. Romanowski M, Łukianowicz C, Sutowska M, et al (2021) Assessment of the Technological Quality of X5CRNI18-10 Steel Parts after Laser and Abrasive Water Jet Cutting Using Synthetic Index of Technological Quality. Materials 14:4801. https://doi.org/10.3390/ma14174801
16. Bachmann AL, Hanrahan B, Dickey MD, Lazarus N (2022) Self-Folding PCB Kirigami: Rapid Prototyping of 3D Electronics via Laser Cutting and Forming. ACS Applied Materials & Interfaces 14:14774–14782. https://doi.org/10.1021/acsami.2c01027

17. Najjar IMR, Sadoun AM, Abd Elaziz M, et al (2022) Predicting kerf quality characteristics in laser cutting of basalt fibers reinforced polymer composites using neural network and chimp optimization. Alexandria Engineering Journal 61:11005–11018. https://doi.org/10.1016/j.aej.2022.04.032
18. Aumnate C, Pongwisuthiruchte A, Pattananuwat P, et al. Fabrication of ABS/Graphene Oxide Composite Filament for Fused Filament Fabrication (FFF) 3D Printing. Advances in Materials Science and Engineering. 2018;2018:1–9.
19. Kechagias J, Chaidas D, Vidakis N, et al (2022) Key parameters controlling surface quality and dimensional accuracy: a critical review of FFF process. Mater Manuf Process 37:963–984. https://doi.org/10.1080/10426914.2022.2032144
20. Chaidas D, Kechagias JD (2022) An investigation of PLA/W parts quality fabricated by FFF. Materials and Manufacturing Processes 37:582–590. https://doi.org/10.1080/10426914.2021.1944193
21. Tsiolikas A, Mikrou T, Vakouftsi F, et al. Robust design application for optimizing ABS fused filament fabrication process: A case study. IOP Conf Ser: Mater Sci Eng. 2019;564:012021.
22. Kechagias JD, Zaoutsos SP, Chaidas D, Vidakis N (2022) Multi-parameter optimization of PLA/Coconut wood compound for Fused Filament Fabrication using Robust Design. Int J Adv Manuf Technol 119:4317–4328. https://doi.org/10.1007/s00170-022-08679-2
23. Fountas NA, Kechagias JD, Manolakos DE, Vaxevanidis NM (2020) Single and multi-objective optimization of FDM-based additive manufacturing using metaheuristic algorithms. Procedia Manuf 51:740–747. https://doi.org/10.1016/ j.promfg.2020.10.104
24. Mushtaq RT, Wang Y, Rehman M, et al. State-Of-The-Art and Trends in CO_2 Laser Cutting of Polymeric Materials—A Review. Materials. 2020;13.
25. Ayrilmis N, Kariz M, Kwon JH, et al. Effect of printing layer thickness on water absorption and mechanical properties of 3D-printed wood/PLA composite materials. The International Journal of Advanced Manufacturing Technology. 2019; 102:2195–2200.
26. Ecker JV, Haider A, Burzic I, et al. Mechanical properties and water absorption behaviour of PLA and PLA/wood composites prepared by 3D printing and injection moulding. Rapid Prototyping Journal. 2019; 25:672–678.
27. Chakule RR, Chaudhari SS, Talmale PS (2021) Modelling and optimisation of nanocoolant minimum quantity lubrication process parameters for grinding performance. International Journal of Experimental Design and Process Optimisation 6:333. https://doi.org/10.1504/IJEDPO.2021.123111
28. Malomo BO, Oladejo KA, Fadairo AA, et al (2019) Multi-objective machining parameter optimisation of aluminium alloy 6063 by the Taguchi-artificial neural network/genetic algorithm approach. International Journal of Experimental Design and Process Optimisation 6:146. https://doi.org/10.1504/IJEDPO.2019.101720
29. Kusuma AI, Huang Y-M (2022) Product quality prediction in pulsed laser cutting of silicon steel sheet using vibration signals and deep neural network. Journal of Intelligent Manufacturing. https://doi.org/10.1007/s10845-021-01881-1
30. Baronti L, Michalek A, Castellani M, et al (2022) Artificial neural network tools for predicting the functional response of ultrafast laser textured/structured surfaces. The International Journal of Advanced Manufacturing Technology 119:3501–3516. https://doi.org/10.1007/s00170-021-08589-9
31. Dhar AR, Gupta D, Roy SS, Lohar AK (2022) Forward and backward modeling of direct metal deposition using metaheuristic algorithms tuned artificial neural network and extreme gradient boost. Progress in Additive Manufacturing. https://doi.org/10.1007/s40964-021-00251-w
32. Tani S, Kobayashi Y (2022) Ultrafast laser ablation simulator using deep neural networks. Scientific Reports 12:5837. https://doi.org/10.1038/s41598-022-09870-x